Nanoscale

View Online
Dynamic Article Links

Cite this: *Nanoscale*, 2011, **3**, 3040

www.rsc.org/nanoscale

FEATURE ARTICLE

Cu_2ZnSnS_4 nanocrystals and graphene quantum dots for photovoltaics

Jun Wang,[a] Xukai Xin[ab] and Zhiqun Lin*[ab]

Received 27th April 2011, Accepted 18th May 2011
DOI: 10.1039/c1nr10425j

Semiconductor quantum dots exhibit great potential for applications in next generation high efficiency, low cost solar cells because of their unique optoelectronic properties. Cu_2ZnSnS_4 (CZTS) nanocrystals and graphene quantum dots (GQDs) have recently received much attention as building blocks for use in solar energy conversion due to their outstanding properties and advantageous characteristics, including high optical absorptivity, tunable bandgap, and earth abundant chemical composition. In this Feature Article, recent advances in the synthesis and utilization of CZTS nanocrystals and colloidal GQDs for photovoltaics are highlighted, followed by an outlook on the future research efforts in these areas.

1. General introduction

Solar energy has been considered as one of the most promising next generation energy resources due to its fully renewable nature, infinite power, and limited impacts to the environment. Single crystal silicon solar cells that are commercially available have a production cell efficiency of 15%.[1] However, the use of silicon-based solar cells is limited due to their lack of flexibility, high cost of manufacturing and installation, and heavy weight, regardless of their high solar-to-electric energy conversion efficiency. In this context, several attractive alternatives to silicon-based solar cells have emerged to achieve low cost, high performance photovoltaics, including organic solar cells,[2–6] dye-sensitized solar cells,[7,8] and quantum dot solar cells.[9,10]

Semiconductor nanocrystals, also known as quantum dots (QDs), promise new opportunities for use in solar cells due to their tunable band edge, efficient optical absorption, and multiple exciton generation capability.[11–19] In an individual QD, the motion of excitons (*i.e.*, pairs of conduction band electrons

[a]*Department of Materials Science and Engineering, Iowa State University, Ames, IA, 50011, USA*
[b]*School of Materials Science and Engineering, Georgia Institute of Technology, Atlanta, GA, 30332, USA. E-mail: zqlin@iastate.edu and zhiqun.lin@mse.gatech.edu; Web: http://zqlin.public.iastate.edu*

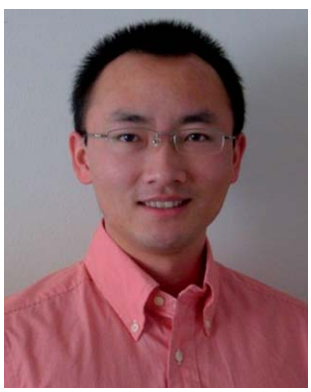

Jun Wang

Jun Wang received the BS degree in Polymer Science and Engineering from University of Science & Technology of China (USTC) in 2005. After that he joined Prof. Zhiqun Lin's group at Iowa State University and received his PhD degree in Materials Science and Engineering in 2009. His graduate work involved synthesis and application of functional nanostructures, including synthesis of colloidal nanocrystals, electrochemical anodization, and nanostructured solar cells. He is the recipient of MRS graduate silver award at the MRS meeting in spring 2010. He is currently a postdoctoral researcher at National Renewable Energy Laboratory in Golden, Colorado. His research interests include synthesis of functional nanostructures, energy storage, energy conversion, and advanced characterization techniques.

Xukai Xin

Xukai Xin received the BS degree in Mathematics and Physics in 2006 and the Master degree in Materials Science and Engineering in 2009; both were from Tsinghua University, Beijing, China. After that he joined Prof. Zhiqun Lin's group at Iowa State University as a PhD student. Currently, he is working on the synthesis of photovoltaic materials and fabrication of photovoltaic devices. His research interests include dye- and quantum dot-sensitized solar cells, quantum dots synthesis, photoactive layer and electrode materials, up-conversion materials, and modeling of light harvesting in solar cells.

and valence band holes) is confined in three spatial directions. Theoretical calculation shows that as many as seven excitons can be generated upon absorption of one photon by QDs at a certain energy level,[18] and an ideal power conversion efficiency (PCE) higher than 40% is expected in QD solar cells.[11,20]

Because of its near-optimum bandgap, earth abundant chemical composition, and high absorption coefficient, Cu_2ZnSnS_4 (CZTS) has attracted considerable attention and been considered as one of the most promising photovoltaic materials.[21–28] In addition to the quantum confinement effect in an individual nanocrystal, colloidal CZTS nanocrystals possess excellent solution processability, making it possible to capitalize on low cost solution-based fabrication techniques, such as spray deposition,[24,29] spin coating,[2,6] drop casting,[22] *etc.* to prepare thin film solar cell devices.

Research on graphene, a single atomic layer of graphite, has undergone rapid development over the past years due to its promising potential to be utilized for next generation electronic devices.[30–42] Most notably, the 2010 Nobel Prize in Physics was awarded to Andre Geim and Konstantin Novoselov for their groundbreaking experiments regarding the two-dimensional material graphene, signifying the scientific and technological importance of graphene. Graphene has zero bandgap and infinite exciton Bohr radius,[32] thus it is possible to achieve quantum confinement in graphene with any finite size, *i.e.*, graphene quantum dots (GQDs). GQDs have a size dependent bandgap and large optical absorptivity,[42,43] making them particularly interesting building blocks for solar energy conversion. Preparation of colloidal GQDs with increased solubility in common solvents is of key importance to fabricate GQD-based solar cells *via* inexpensive solution-based processing.

It is worth noting that we make no attempt to cover the QD solar cell literature here but refer the reader to several comprehensive reviews contributed by leading scientists in this field.[9,44–49] Instead, this Feature Article seeks to highlight recent advances in the synthesis and utilization of Cu_2ZnSnS_4 (CZTS) nanocrystals and colloidal graphene quantum dots (GQDs) for photovoltaic applications. An outlook on the future research efforts in these areas is provided.

Zhiqun Lin

Zhiqun Lin received the BS degree in Materials Chemistry from Xiamen University, Xiamen, China in 1995, the Master degree in Macromolecular Science from Fudan University, Shanghai, China in 1998, and the PhD degree in Polymer Science and Engineering from University of Massachusetts, Amherst in 2002. From November 2002 to July 2004 he was a postdoctoral associate in the Department of Materials Science and Engineering at University of Illinois, Urbana-Champaign. He joined the Department of Materials Science and Engineering at Iowa State University as an Assistant Professor in 2004 and was promoted to Associate Professor in 2010. He moved to Georgia Institute of Technology in 2011. His research interests include solar cells, conjugated polymers, quantum dots (rods), polymer-based nanocomposites, block copolymers, polymer blends, hierarchical structure formation and assembly, phase equilibrium and phase separation kinetics, surface and interfacial properties, ferroelectric nanocrystals, multiferroic nanocrystals, thermoelectric nanocrystals, multifunctional nanocrystals. He is a recipient of an NSF Career Award and a 3M Non-Tenured Faculty Award, and an invited participant at the National Academy of Engineering's (NAE) 2010 US Frontiers of Engineering Symposium (US FOE).

2. Cu_2ZnSnS_4 (CZTS) nanocrystals for solar cells

In recent years, low cost, environmentally friendly CZTS has sparkled tremendous research interest. It has a near-optimum direct bandgap energy of ~1.5eV and a large absorption coefficient (>10^4 cm^{-1}). Sn and Zn are naturally abundant in the Earth's crust and have very low toxicity.[21] Most work on CZTS-based solar cells has centered on the bulk thin films, which are usually deposited on a desired substrate by sputtering,[50] sulfurization of metallic layer,[51,52] multisource evaporating,[53] and spray pyrolysis,[54,55] *etc.*, and a PCE up to 6.7% has been achieved in CZTS thin film solar cells.[56] Very recently, IBM scientists achieved a record of 9.6% PCE in CZTS solar cells using a solution-based mixture by spin coating and heat treatments.[28]

Recent advances in the colloidal synthesis of high quality nanocrystals with remarkable solubility in common solvents have provided a means of fabricating functional nanodevices using solution processing techniques. To this end, it is quite intriguing to synthesize colloidal CZTS nanocrystals and exploit them to produce inexpensive, high efficiency solar cells through a scalable solution processing fabrication.[22–27]

2.1. Synthesis of CZTS nanocrystals

High quality CZTS nanocrystals have been successfully prepared by hot-injection thermolysis.[22–24] Fig. 1 shows the transmission electron microscopy (TEM) and X-ray powder diffraction (XRD) of as-synthesized CZTS nanocrystals. Briefly, copper acetylacetonate, zinc acetylacetonate, and tin acetylacetonate with a molar ratio of 2 : 1 : 1 were first dissolved in oleylamine upon heating under Ar, to which sulfur dissolved in oleylamine was rapidly injected at 225 °C, the reaction was carried out at this temperature for 1 h.

After cooling down to room temperature, a mixed solvent of ethanol/toluene was used to purify the resulting nanocrystals. The final product can be dispersed in various organic solvents (*e.g.*, toluene, hexane, and chloroform). Oleylamine served as both high boiling point solvent and surfactant to prevent the aggregation of nanocrystals and provide excellent solubility. High resolution TEM characterization showed that as-synthesized CZTS nanocrystals were highly crystalline (inset in Fig. 1a), and XRD measurement revealed that CZTS nanocrystals have tetragonal phase (PDF # 026-0575) (Fig. 1b).

It is noteworthy that the XRD profiles of stoichiometric tetragonal Cu_2SnS_3 and cubic ZnS are very similar to that of tetragonal CZTS as shown in Fig. 2.[23] Thus, it is necessary to determine the phase purity in as-synthesized CZTS nanocrystals. In addition to using energy dispersive X-ray spectroscopy (EDS)

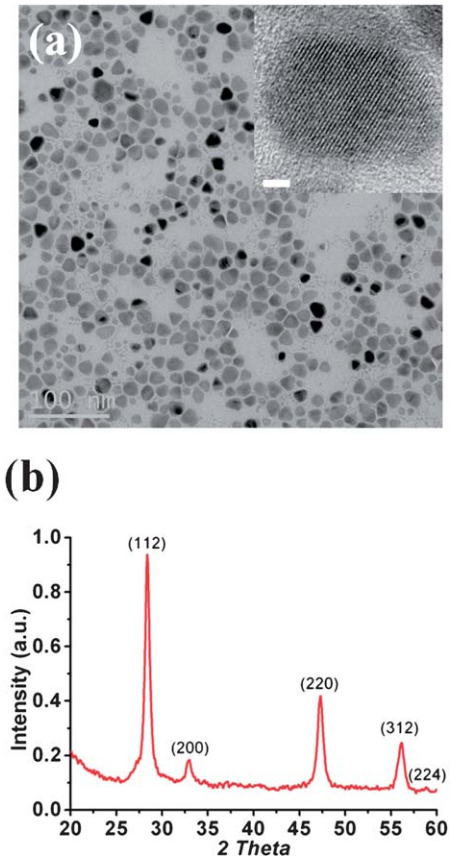

Fig. 1 (a) TEM image of as-synthesized CZTS nanocrystals; scale bar = 100 nm. Inset shows a high resolution TEM image of an individual nanocrystal exhibiting the crystalline lattice; scale bar = 2 nm. (b) X-ray powder diffraction pattern of CZTS nanocrystals. The characteristic peaks can be indexed to tetragonal CZTS (PDF # 026-0575). (Results obtained from Zhiqun Lin Research Group at Iowa State University.)

analysis to confirm the stoichiometry of elements and X-ray photoelectron spectroscopy (XPS) to determine the oxidation states of each element, differential thermal analysis (DTA) can be used to rule out the possibility that the obtained nanocrystals are a mixture of Cu_2SnS_3 : ZnS phases[23] as these materials have different melting transition temperatures. Investigation on the experimental conditions revealed that the reaction temperature played a key role in synthesizing CZTS nanoparticles, *i.e.*, a temperature higher than 240 °C yielded a pure CZTS crystal phase while a secondary phase of CuS was formed at a temperature lower than 180 °C.[27]

The obtained CZTS nanocrystals exhibited strong optical absorption from visible to near IR region (Fig. 3). The bandgap of CZTS nanocrystals determined from the absorbance *versus* photon energy plot was calculated to be 1.5 eV, which is consistent with the value of bulk CZTS and near-optimum for the purpose of realizing photovoltaic solar conversion in a single bandgap device.[22–25]

2.2. CZTS nanocrystals based solar cells

Solution-based processing techniques, such as spray depositing[24] and drop casting,[22,25,26] have been utilized to yield CZTS thin film solar cells by coating the CZTS nanocrystal ink on gold (Au) or

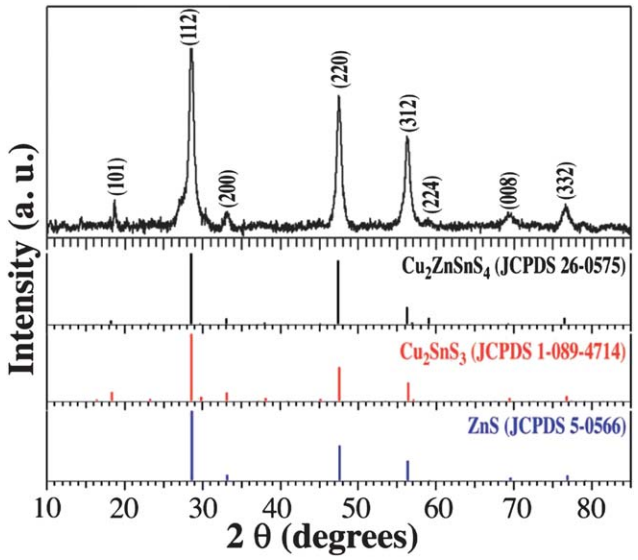

Fig. 2 XRD pattern of CZTS nanocrystals. The peaks are indexed to tetragonal CZTS. The standard XRD patterns of CZTS, CTS, and ZnS are shown below in black, red, and blue lines, respectively, indicating that three materials have similar diffraction patterns. (Reprinted with permission from ref. 23, Riha *et al.*, *J. Am. Chem. Soc.*, 2009, **131**, 12054; copyright© The American Chemical Society.)

molybdenum (Mo) modified soda lime glass. A CdS buffer layer was then deposited on top of CZTS thin film by chemical bath deposition, followed by a sputtering deposition of the top contact (*e.g.*, ZnO/ITO). Selenization was usually carried out on the CZTS thin film by annealing under selenium vapor to partially replace sulfur and enhance the grain growth,[22,25] which effectively improved the device performance.[57] Additionally, the formation of a $MoSe_2$ interfacial layer at the CZTS/Mo interface was critical in facilitating a quasi-ohmic electrical contact.[28,58] Initial trials on CZTS nanocrystal-based thin film solar cells unfortunately led to a very low PCE (less than 1%), due primarily to poorly optimized synthesis of CZTS nanocrystals and device fabrication.[22,24]

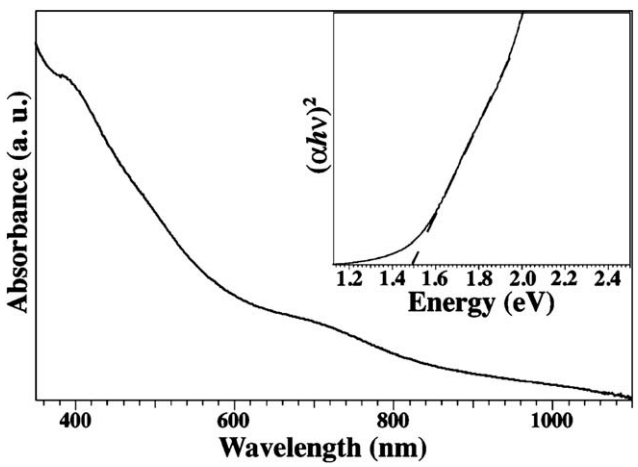

Fig. 3 UV-Vis absorption spectrum of CZTS nanocrystals. The calculated bandgap of 1.5 eV is shown in the inset. (Reprinted with permission from ref. 23, Riha *et al.*, *J. Am. Chem. Soc.*, 2009, **131**, 12054; copyright© The American Chemical Society.)

More recently, Guo *et al.* successfully addressed the efficiency-limiting challenges and obtained a high PCE of 7.2% from selenized CZTS nanocrystal thin films.[25] A cross-section SEM image of a typical CZTS nanocrystal-based thin film solar cell is shown in Fig. 4, in which large densely packed grains in CZTS film were clearly evident.[25] To fabricate the device, CZTS nanocrystals dispersed in hexanethiol were directly deposited on Mo-coated soda lime glass to form a densely packed nanocrystal thin film by the 'knife coating' technique with scotch tape used as a spacer. Dithiol molecules served as a crosslinking agent to promote the formation of dense nanocrystal film.[25,27] The majority of sulfur was replaced with selenium by annealing the thin film under selenium vapor at 500 °C, resulting in a final Cu/(Zn + Sn) ratio of 0.79 and a Zn/Sn ratio of 1.11. Chemical bath deposition of CdS and RF sputtering of ZnO/ITO were subsequently performed to fulfill the device fabrication. The other key factor attributed to the greatly improved device performance was the optimized chemical composition in CZTS nanocrystals, *i.e.*, an overall copper poor and zinc rich composition, which has been recognized as an optimal condition for maximizing the CZTS solar cell performance.[59]

The *J–V* characteristics and external quantum efficiency (EQE) of a CZTS nanocrystal thin film solar cell after selenization are shown in Fig. 5. A PCE of 7.2% under AM 1.5 illumination and an EQE as high as 90% in the visible range were achieved.[25] It was anticipated that the device performance could be further enhanced by improving the sheet resistance of Mo and ITO layers and optimizing the thickness of light absorber layer.

Since selenization in CZTS nanocrystal solar cells is quite necessary, it is of particular interest to directly synthesize CZTSe or CZTSSe nanocrystals for the deposition of a light absorbing layer. Recent progress in nanocrystals synthesis has led to high quality CZTSe nanocrystals using a modified procedure for the preparation of CZTS nanocrystals.[60–62] Notably, utilizing selenium in trioctylphosphine (TOP-Se) as a selenium source in the hot-injection synthesis, nearly monodisperse CZTSe nanocrystals have been obtained.[62]

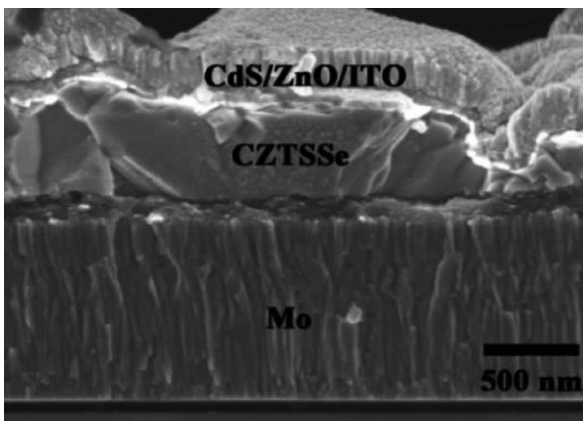

Fig. 4 Cross-section field emission SEM image of a CZTSSe thin film solar cell. (Reprinted with permission from ref. 25, Guo *et al.*, *J. Am Chem. Soc.*, 2010, **132**, 17384; copyright© The American Chemical Society.)

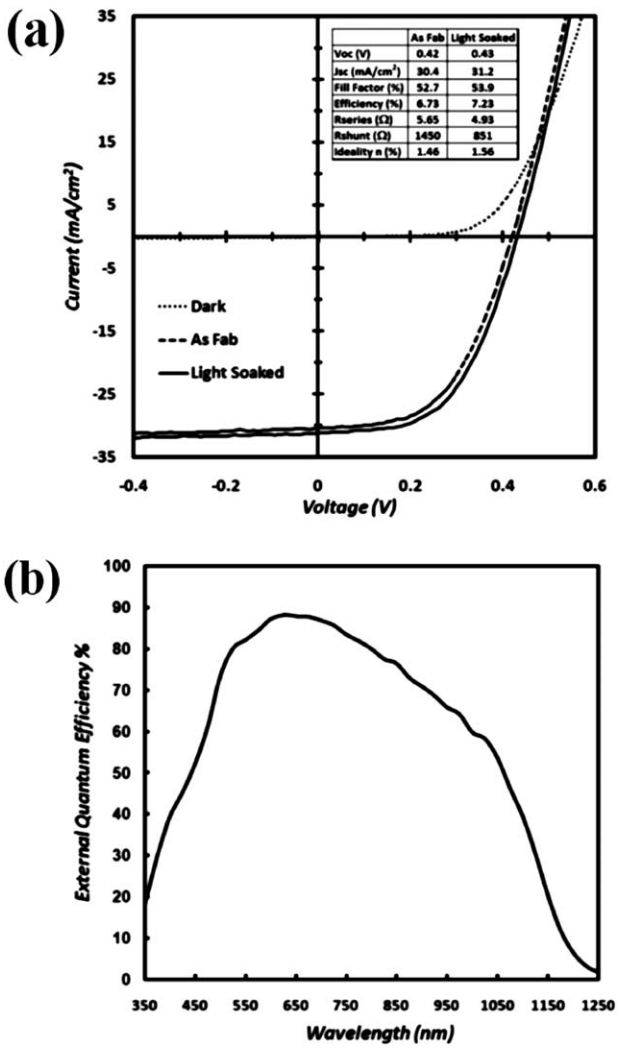

Fig. 5 (a) Characteristic *J–V* curves of CZTSSe solar cells measured in the dark, as-fabricated, and after light soaking for 15 min under AM 1.5 illumination, respectively. (b) External quantum efficiency (EQE) of the CZTSSe solar cell. (Reprinted with permission from ref. 25, Guo *et al.*, *J. Am Chem. Soc.*, 2010, **132**, 17384; copyright© The American Chemical Society.)

3. Graphene quantum dot-based solar cells

Graphene quantum dots (GQDs) with size dependent bandgap and large optical absorptivity are promising candidate materials for use in solar cells and electronic devices.[41,63–72] However, the synthesis of colloidal GQDs with excellent solubility in common solvents is far less developed due most likely to the insufficient surface protection to overcome strong intergraphene attraction, which usually leads to the formation of graphite particles.[73] To date, two approaches have been exploited to prepare colloidal GQDs, *i.e.*, top-down cutting of graphene sheets and bottom-up oxidative condensation reactions as will be discussed below.

3.1. Synthesis of colloidal GQDs

Both top-down and bottom-up approaches have been applied to synthesize GQDs with tunable size. Top-down approach refers to

the cutting of graphene sheets into GQDs, while bottom-up method involves the synthesis of graphene moieties containing a certain number of conjugated carbon atoms.

Pan *et al.* developed a hydrothermal route to cutting graphene sheets into GQDs, exhibiting blue luminescence.[74] Briefly, graphene sheets were first obtained by deoxidation of graphene oxide sheets, followed by controlled oxidation in a mixture of sulfuric acid and nitric acid under mild ultrasonication. The oxidized graphene sheets were then collected and cut into GQDs under hydrothermal conditions in a Teflon lined autoclave at elevated temperature. The obtained GQDs had an average diameter of 9.6 nm (Fig. 6a) consisting of 1–3 layer graphene, and exhibited a quantum yield of 6.9% using quinine sulfate as a reference. The cutting mechanism involved the complete breakup of mixed epoxy chains composed of fewer epoxy groups and more carbonyl groups under hydrothermal conditions.

Later, Li *et al.* reported an electrochemical means of synthesizing green-luminescent GQDs and utilized the resulting GQDs as electron acceptors in GQD–P3HT hybrid thin film solar cells.[75] GQDs were formed by electrochemical oxidation of a graphene electrode in phosphate buffer solution. The obtained GQDs had a uniform size of 3–5 nm (Fig. 6b) and exhibited green luminescence. The oxygen containing groups on the surface of GQDs provided an aqueous solubility and facilitated further surface functionalization. Similar to GQDs obtained under hydrothermal conditions,[74] GQDs produced by electrochemical oxidation were made of 1–3 graphene layers attributed to strong intergraphene attraction.

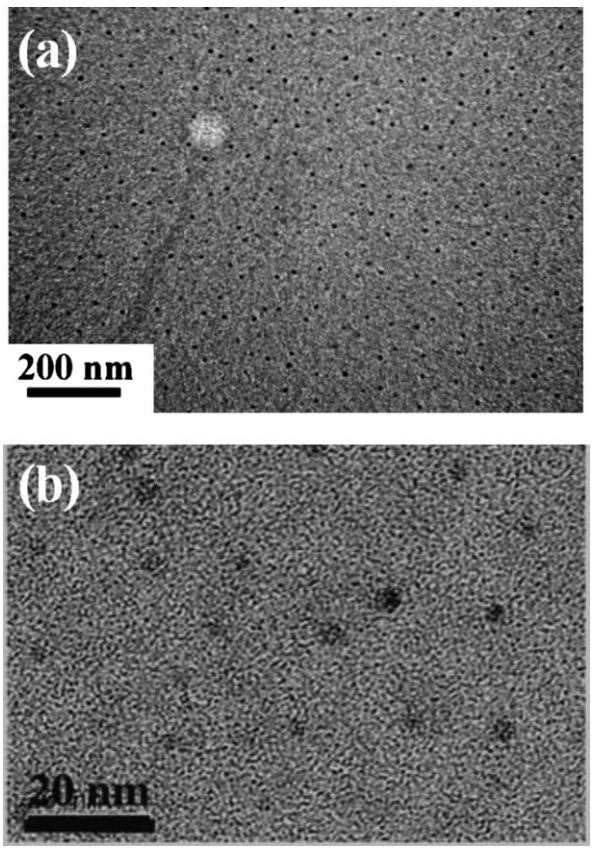

Fig. 6 TEM images of (a) blue-luminescent GQDs produced by hydrothermally cutting graphene sheets and (b) green-luminescent GQDs obtained by electrochemical approach. (Reprinted with permission from ref. 74 and 75, Pan *et al.*, *Adv. Mater.*, 2010, **22**, 734 and Li *et al.*, *Adv. Mater.*, 2011, **23**, 776; copyright© Wiley).

As for the bottom-up approach, GQDs have been successfully synthesized *via* solution chemistry by oxidative condensation of aryl groups (Scholl reaction).[43,73,76–82] It has been demonstrated that intramolecular variation is useful for the synthesis of large polycyclic aromatic hydrocarbons (PAHs) from dendritic arene precursors.[73,81,82] GQDs with up to 222 conjugated carbon atoms have been successfully prepared, however the solubility of such GQDs was unfortunately low and they exhibited a tendency to aggregate due to strong intergraphene attraction. Very recently, Li *et al.* creatively applied 2′, 4′, 6′-triakyl phenyl groups as stabilizing agent to form 3-D protection at the edge of graphene moieties, resulting in GQDs with tunable size and high colloidal stability.[43,80] The formation of 3-D protection was attributed to the strong covalent binding and twisted phenyl groups due to crowdedness at the edge of graphene moieties. Fig. 7a depicts GQDs containing 168, 132, and 170 conjugated carbon atoms, respectively. The mechanism for 3-D protection by twisted ligands that covalently attach to the edge of GQDs is illustrated in Fig. 7b.

A solution-based synthetic route to GQDs was recently developed by Yan *et al.*[43] Synthesis of GQDs was based on the oxidation of polyphenylene dendritic precursors (1, 2, and 3 in Fig. 8), which were prepared *via* a stepwise solution chemistry shown in the scheme below (Fig. 8).[43]

Trialkyl phenyl groups covalently attached to the edge of graphene moieties rendered them with excellent solubility in common organic solvents, such as toluene, THF, chloroform, *etc.* Isotope-resolved mass spectroscopy with mild ionization methods (*e.g.*, MALDI-TOF) was found to be the most effective means of identifying GQDs, and the results suggested that GQDs had high uniformity in size. Dynamic light scattering (DLS) on GQDs showed an average size more than twice as high as that obtained from molecular modeling (*i.e.*, 13.5 nm *versus* 5 nm for GQDs with 168 conjugated carbon atoms), indicating oligomerization of GQDs in solution due to residual intergraphene attraction, which also explained why conventional liquid NMR spectroscopy failed in characterizing GQDs.[43,80]

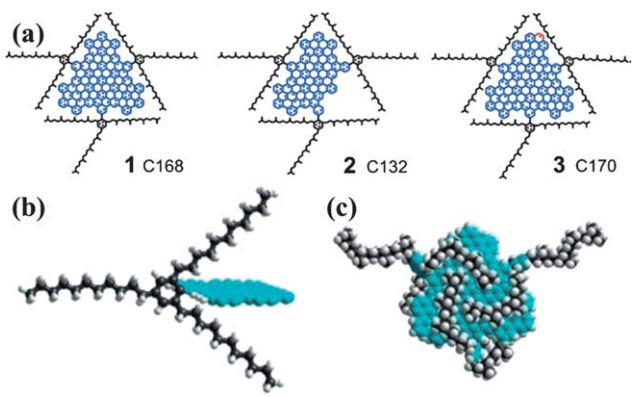

Fig. 7 (a) Schemes of colloidal GQDs with tunable size. (b) and (c) Strategies to make GQDs soluble. (Reprinted with permission from ref. 43 and 80, Yan *et al.*, *J. Am. Chem. Soc.*, 2010, **132**, 5944 and *Nano Lett.*, 2010, **10**, 1869; copyright© The American Chemical Society.)

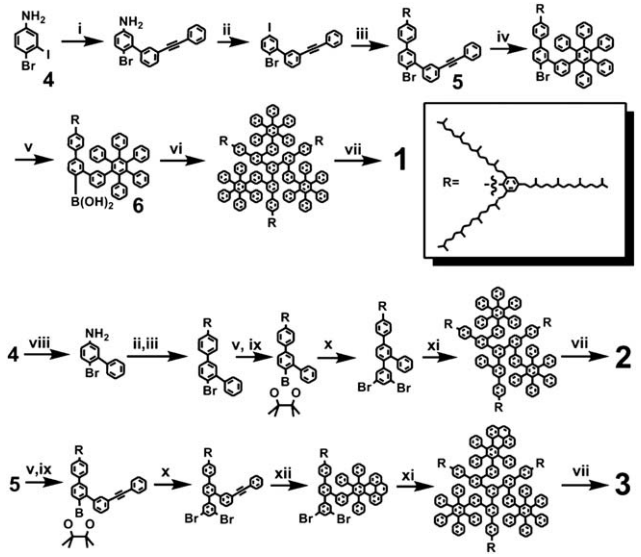

Fig. 8 Synthesis of GQDs *via* a wet chemistry approach. (Reprinted with permission from ref. 43, Yan *et al.*, *J. Am. Chem. Soc.*, 2010, **132**, 5944; copyright© The American Chemical Society.)

Size and shape dependent optical absorption in these GQDs was revealed by UV-Vis absorption measurements (Fig. 9).[43] GQDs with larger size (*i.e.*, 168 and 170 conjugated carbon atoms) showed absorption edges at significantly longer wavelengths than smaller GQDs (*i.e.*, 132 conjugated carbon atoms). This size dependent optical absorption confirmed the quantum confinement in GQDs, and is consistent with the size dependent absorption in other QDs.[83] Notably, these GQDs possessed broad absorption from visible to near IR region, and an absorbance maximum of 1.0×10^5 M^{-1} cm^{-1} was about an order of magnitude larger than conventional ruthenium dyes in dye-sensitized solar cells, suggesting that these GQDs are ideal candidates for photovoltaic applications.[80]

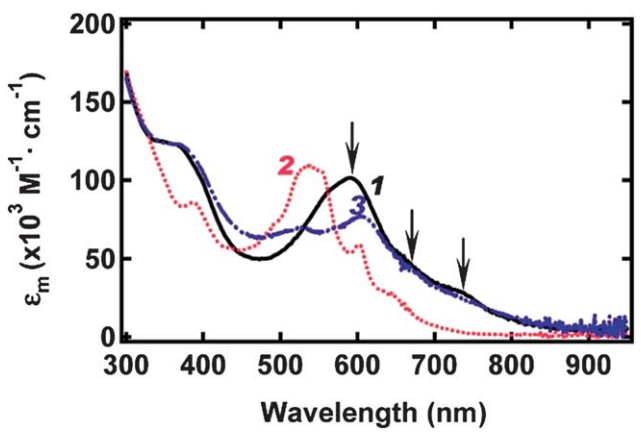

Fig. 9 UV-Vis absorption of colloidal GQDs. α, p, and β bands of GQDs with 168 conjugated carbon atoms are marked by arrows (*i.e.*, **1** in Fig. 7a and 8), from right to left, respectively. (Reprinted with permission from ref. 43, Yan *et al.*, *J. Am. Chem. Soc.*, 2010, 132, 5944; copyright © The American Chemical Society.)

3.2. Photovotaics based on colloidal GQDs

Owing to their attractive optoelectronic properties and solution processability, colloidal GQDs hold the promise of applications in low cost, high performance photovoltaic devices (*e.g.*, organic/inorganic hybrid solar cells and GQD-sensitized solar cells).

Li *et al.* applied colloidal GQDs with green luminescence as an electron collector in conjugated polymer, poly(3-hexylthiophene) (P3HT)-based thin film solar cells.[75] Fig. 10a shows the energy level alignment with a device configuration of ITO/PEDOT:PSS/P3HT:GQDs/Al, in which GQDs (c = 10 wt%) provided an effective interface for charge separation and a pathway for electron transport, as clearly evidenced by a greatly increased photocurrent as compared to the device fabricated with P3HT only (Fig. 10b). The device performance was further enhanced after thermal annealing, and an overall PCE of 1.28% was achieved. Further improvement in performance is expected by optimizing the device fabrication.

Recent work by Yan *et al.* showed that GQDs have high optical absorptivity and nearly optimized absorption in the visible and near IR region. Moreover, the calculated energy level

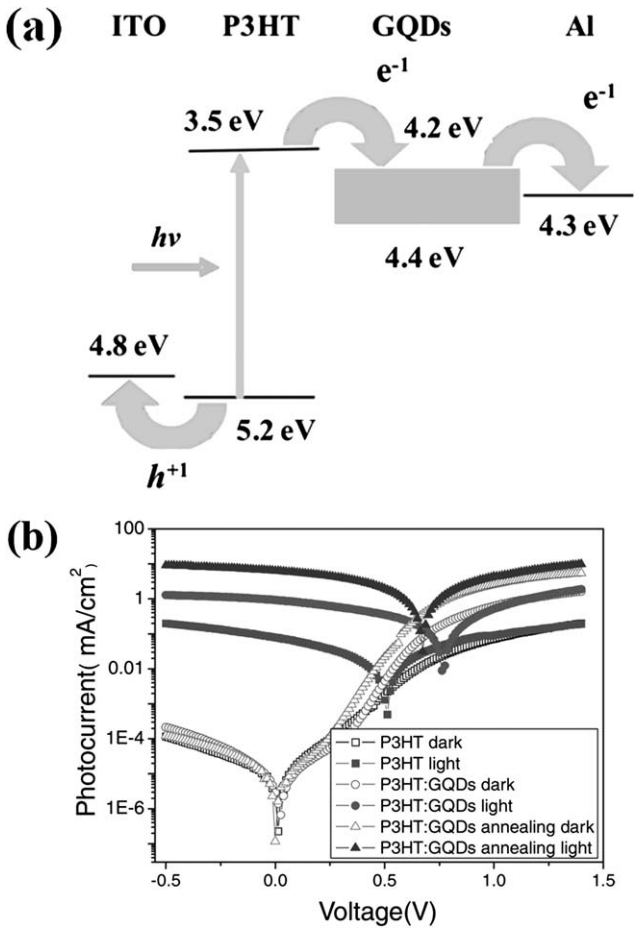

Fig. 10 (a) Energy level alignment diagram of the ITO/PEDOT:PSS/P3HT:GQDs/Al solar cell device. (b) *J–V* curves of the ITO/PEDOT:PSS/P3HT/Al, ITO/PEDOT:PSS/P3HT:GQDs/Al and ITO/PEDOT:PSS/P3HT:GQDs/Al devices after annealed at 140 °C for 10 min; single log scale. (Reprinted with permission from ref. 75, Li *et al.*, *Adv. Mater.*, 2011, **23**, 776; copyright © Wiley.)

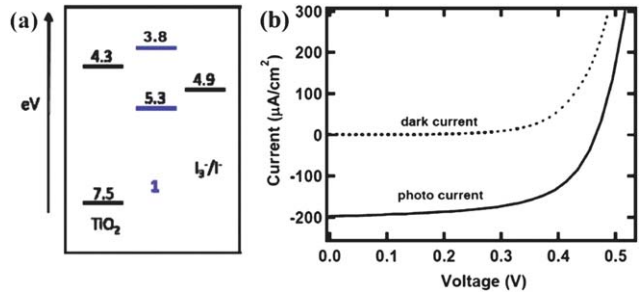

Fig. 11 (a) Calculated energy level alignment. (b) *J–V* characteristics of colloidal GQD-sensitized TiO_2 nanoparticle solar cells. (Reprinted with permission from ref. 80, Yan *et al.*, *Nano Lett.*, 2010, **10**, 1869; copyright© The American Chemical Society.)

in GQDs suggested the possibility of electron injection from GQDs to large bandgap semiconductors (*e.g.*, TiO_2) upon photoexcitation and regeneration of GQDs by accepting an electron from I^- (Fig. 11a).[80] Thus, in conjunction with an earth abundant composition characteristic, GQDs provide unique opportunities for the development of inexpensive, high efficiency GQD-sensitized solar cells by substituting GQDs for metal-organic dyes as photosensitizers. As a proof-of-concept, Yan *et al.* exploited GQDs with 168 conjugated carbon atoms to sensitize a nanocrystalline TiO_2 photoanode and obtained a photocurrent density of 200 μA cm^{-2} under AM 1.5 illumination (Fig. 11b).[80] The low performance was due largely to the low affinity of GQDs to the surface of TiO_2 since no chemical binding was formed as in conventional dye-sensitized solar cells, in which ruthenium dyes are covalently bonded to the TiO_2 surface for much higher optical absorption and faster exciton dissociation.

4. Conclusions and outlook

Rapid development has been witnessed in CZTS nanocrystals and GQDs that may open up new avenues for fabricating inexpensive and scalable next generation solar cells with high photovoltaic performance due to their outstanding optoelectronic properties (large optical absorption of solar irradiation and tunable bandgap) and naturally abundant chemical composition. Previous work on CZTS nanocrystals and GQDs based solar cells has demonstrated promising solar energy conversion. As discussed below, future research efforts towards better controlled synthesis, surface functionalization and novel device fabrication are expected to result in even higher device performance.

4.1. Synthesis of high quality CZTS nanocrystals

Synthesis of high quality CZTS nanocrystals with well controlled size, shape, and chemical composition needs to be further explored. Theoretical simulation shows that the stable chemical potential region for the formation of stoichiometric compound in CZTS is small, and the growth of CZTS under a Cu-poor/Zn-rich condition would be optimal for maximizing device performance.[59,84,85] A recent study on CZTS and CZTSe nanocrystals using advanced electron microscopy showed that these nanoparticles exhibited a broad range of chemical heterogeneity in individual nanoparticles while very good stoichiometric composition was observed with overview measurement.[60] A precise control over the size and shape of CZTS nanocrystals may also benefit the self-organization of nanocrystals into a thin film, thereby leading to high quality thin CZTS films.[86–88]

4.2. Surface engineering on CZTS nanocrystals

Effective surface engineering of CZTS nanocrystals is highly desirable for forming higher quality CZTS nanocrystal thin films and thus high efficiency solar cells. The use of organic ligands provides nanocrystals with excellent solubility in organic solvents, thus allowing for inexpensive, large scale solution-based processing. However, it may be difficult to remove all the ligands by thermal annealing as organic residues in the CZTS film may act as defects for charge accumulation and material degradation. Recent advances in colloidal chemistry have brought about the preparation of a series of inorganic ligands (*e.g.*, $Sn_2S_6^{4-}$, SnS_4^{4-}, $SnTe_4^{4-}$, AsS_3^{3-}, and MoS_4^{2-}), which not only render nanocrystals with essential solubility but also can be transformed into semiconductor solids upon thermal treatment.[88–91] The use of inorganic ligands for surface capping of CZTS nanocrystals may yield much higher film quality, and ultimately higher photovoltaic performance.

4.3. Surface engineering on GQDs

Both top-down and bottom-up approaches have been implemented for the synthesis of GQDs. In contrast, surface engineering of GQDs is less developed. In GQD-sensitized solar cells, the poor affinity between GQDs and TiO_2 surface was responsible for quite low photocurrent. Very recently, Hamilton *et al.* have successfully introduced functional groups on GQDs by creating carbon–carbon covalent bonds between functional molecules and GQDs and demonstrated that the orientation of GQDs on the polar surface can be determined by the chemical functionalization on GQDs.[77] There is a myriad of literature on the functionalization of carbon nanotube by functional ligands.[92–102] It will be of great interest to extend these surface functionalization techniques to GQDs.

4.4. Novel nanostructured TiO_2 for GQD-sensitized solar cells

A wide diversity of nanostructured TiO_2 has been successfully produced, including mesoporous TiO_2 thin films,[103,104] TiO_2 nanotube arrays,[105–109] and TiO_2 nanowires.[110,111] Of particular interest are highly ordered TiO_2 nanotube arrays fabricated by electrochemical anodization that have been extensively investigated in the last decade for potential applications in dye-sensitized solar cells,[112–117] gas sensors,[118–120] water splitting,[113,121–123] photocatalysts,[124,125] and cell separation.[126,127] Vertically aligned TiO_2 nanotubes not only provide high surface area for large volume of reaction sites but also facilitate efficient vectorial charge transport along the nanotube. Recently, by impregnating TiO_2 nanotube arrays with ruthenium dye as the sensitizer in conjunction with rational surface engineering on TiO_2 surface, an overall PCE of more than 7% has been achieved.[114,117] Thus, it would be intriguing to integrate colloidal GQDs into highly ordered TiO_2 nanotube arrays and promising device performance can be expected. Similar to other quantum dot-sensitized solar cells (*e.g.*, CdSe), achieving sufficient infiltration of GQDs

inside TiO_2 nanotubes, optimizing electronic interaction between GQDs and TiO_2, and utilizing appropriate hole transport electrolyte, will be main practical challenges for GQD-sensitized solar cells and require a great deal of attention.

Acknowledgements

We gratefully acknowledge support from the DOE Ames Laboratory Seed Funding.

Notes and references

1 P. V. Kamat, *J. Phys. Chem. C*, 2008, **112**, 18737–18753.
2 W. U. Huynh, J. J. Dittmer and A. P. Alivisatos, *Science*, 2002, **295**, 2425–2427.
3 J. Peet, A. J. Heeger and G. C. Bazan, *Acc. Chem. Res.*, 2009, **42**, 1700–1708.
4 I. Gur, N. A. Fromer, C. P. Chen, A. G. Kanaras and A. P. Alivisatos, *Nano Lett.*, 2007, **7**, 409–414.
5 L. M. Chen, Z. R. Hong, G. Li and Y. Yang, *Adv. Mater.*, 2009, **21**, 1434–1449.
6 I. Gur, N. A. Fromer, M. L. Geier and A. P. Alivisatos, *Science*, 2005, **310**, 462–465.
7 M. Gratzel, *Nature*, 2001, **414**, 338–344.
8 B. Oregan and M. Gratzel, *Nature*, 1991, **353**, 737–740.
9 A. J. Nozik, M. C. Beard, J. M. Luther, M. Law, R. J. Ellingson and J. C. Johnson, *Chem. Rev.*, 2010, **110**, 6873–6890.
10 A. J. Nozik, *Phys. E.*, 2002, **14**, 115–120.
11 M. C. Hanna and A. J. Nozik, *J. Appl. Phys.*, 2006, **100**, 074510.
12 R. J. Ellingson, M. C. Beard, J. C. Johnson, P. R. Yu, O. I. Micic, A. J. Nozik, A. Shabaev and A. L. Efros, *Nano Lett.*, 2005, **5**, 865–871.
13 J. E. Murphy, M. C. Beard, A. G. Norman, S. P. Ahrenkiel, J. C. Johnson, P. R. Yu, O. I. Micic, R. J. Ellingson and A. J. Nozik, *J. Am. Chem. Soc.*, 2006, **128**, 3241–3247.
14 R. D. Schaller, V. M. Agranovich and V. I. Klimov, *Nat. Phys.*, 2005, **1**, 189.
15 R. D. Schaller and V. I. Klimov, *Phys. Rev. Lett.*, 2004, **92**, 186601.
16 R. D. Schaller, M. A. Petruska and V. I. Klimov, *Appl. Phys. Lett.*, 2005, **87**, 253102.
17 R. D. Schaller, M. Sykora, S. Jeong and V. I. Klimov, *J. Phys. Chem. B*, 2006, **110**, 25332–25338.
18 R. D. Schaller, M. Sykora, J. M. Pietryga and V. I. Klimov, *Nano Lett.*, 2006, **6**, 424.
19 A. Shabaev, A. L. Efros and A. J. Nozik, *Nano Lett.*, 2006, **6**, 2856–2863.
20 P. R. Yu, K. Zhu, A. G. Norman, S. Ferrere, A. J. Frank and A. J. Nozik, *J. Phys. Chem. B*, 2006, **110**, 25451–25454.
21 C. Wadia, A. P. Alivisatos and D. M. Kammen, *Environ. Sci. Technol.*, 2009, **43**, 2072.
22 Q. J. Guo, H. W. Hillhouse and R. Agrawal, *J. Am. Chem. Soc.*, 2009, **131**, 11672.
23 S. C. Riha, B. A. Parkinson and A. L. Prieto, *J. Am. Chem. Soc.*, 2009, **131**, 12054.
24 C. Steinhagen, M. G. Panthani, V. Akhavan, B. Goodfellow, B. Koo and B. A. Korgel, *J. Am. Chem. Soc.*, 2009, **131**, 12554.
25 Q. Guo, G. M. Ford, W. C. Yang, B. C. Walker, E. A. Stach, H. W. Hillhouse and R. Agrawal, *J. Am. Chem. Soc.*, 2010, **132**, 17384–17386.
26 S. C. Riha, S. J. Fredrick, J. B. Sambur, Y. J. Liu, A. L. Prieto and B. A. Parkinson, *ACS Appl. Mater. Interfaces*, 2011, **3**, 58–66.
27 T. Kameyama, T. Osaki, K. Okazaki, T. Shibayama, A. Kudo, S. Kuwabata and T. Torimoto, *J. Mater. Chem.*, 2010, **20**, 5319–5324.
28 T. K. Todorov, K. B. Reuter and D. B. Mitzi, *Adv. Mater.*, 2010, **22**, E156–E159.
29 V. A. Akhavan, B. W. Goodfellow, M. G. Panthani, D. K. Reid, D. J. Hellebusch, T. Adachi and B. A. Korgel, *Energy Environ. Sci.*, 2010, **3**, 1600–1606.
30 J. C. Meyer, A. K. Geim, M. I. Katsnelson, K. S. Novoselov, T. J. Booth and S. Roth, *Nature*, 2007, **446**, 60–63.
31 K. S. Novoselov, A. K. Geim, S. V. Morozov, D. Jiang, M. I. Katsnelson, I. V. Grigorieva, S. V. Dubonos and A. A. Firsov, *Nature*, 2005, **438**, 197–200.
32 A. K. Geim and K. S. Novoselov, *Nat. Mater.*, 2007, **6**, 183–191.
33 S. Pisana, M. Lazzeri, C. Casiraghi, K. S. Novoselov, A. K. Geim, A. C. Ferrari and F. Mauri, *Nat. Mater.*, 2007, **6**, 198–201.
34 F. Schedin, A. K. Geim, S. V. Morozov, E. W. Hill, P. Blake, M. I. Katsnelson and K. S. Novoselov, *Nat. Mater.*, 2007, **6**, 652–655.
35 A. Das, S. Pisana, B. Chakraborty, S. Piscanec, S. K. Saha, U. V. Waghmare, K. S. Novoselov, H. R. Krishnamurthy, A. K. Geim, A. C. Ferrari and A. K. Sood, *Nat. Nanotechnol.*, 2008, **3**, 210–215.
36 M. I. Katsnelson, K. S. Novoselov and A. K. Geim, *Nat. Phys.*, 2006, **2**, 620–625.
37 K. S. Novoselov, E. McCann, S. V. Morozov, V. I. Fal'ko, M. I. Katsnelson, U. Zeitler, D. Jiang, F. Schedin and A. K. Geim, *Nat. Phys.*, 2006, **2**, 177–180.
38 D. C. Elias, R. R. Nair, T. M. G. Mohiuddin, S. V. Morozov, P. Blake, M. P. Halsall, A. C. Ferrari, D. W. Boukhvalov, M. I. Katsnelson, A. K. Geim and K. S. Novoselov, *Science*, 2009, **323**, 610–613.
39 K. S. Novoselov, A. K. Geim, S. V. Morozov, D. Jiang, Y. Zhang, S. V. Dubonos, I. V. Grigorieva and A. A. Firsov, *Science*, 2004, **306**, 666–669.
40 K. S. Novoselov, Z. Jiang, Y. Zhang, S. V. Morozov, H. L. Stormer, U. Zeitler, J. C. Maan, G. S. Boebinger, P. Kim and A. K. Geim, *Science*, 2007, **315**, 1379–1379.
41 L. A. Ponomarenko, F. Schedin, M. I. Katsnelson, R. Yang, E. W. Hill, K. S. Novoselov and A. K. Geim, *Science*, 2008, **320**, 356–358.
42 R. R. Nair, P. Blake, A. N. Grigorenko, K. S. Novoselov, T. J. Booth, T. Stauber, N. M. R. Peres and A. K. Geim, *Science*, 2008, **320**, 1308–1308.
43 X. Yan, X. Cui and L. S. Li, *J. Am. Chem. Soc.*, 2010, **132**, 5944.
44 J. M. Feng, J. J. Han and X. J. Zhao, *Prog. Org. Coat.*, 2009, **64**, 268–273.
45 P. V. Kamat, *J. Phys. Chem. C*, 2008, **112**, 18737–18753.
46 P. V. Kamat, K. Tvrdy, D. R. Baker and J. G. Radich, *Chem. Rev.*, 2010, **110**, 6664–6688.
47 A. Kongkanand, K. Tvrdy, K. Takechi, M. Kuno and P. V. Kamat, *J. Am. Chem. Soc.*, 2008, **130**, 4007–4015.
48 I. Mora-Sero, S. Gimenez, F. Fabregat-Santiago, R. Gomez, Q. Shen, T. Toyoda and J. Bisquert, *Acc. Chem. Res.*, 2009, **42**, 1848–1857.
49 S. Ruhle, M. Shalom and A. Zaban, *ChemPhysChem*, 2010, **11**, 2290–2304.
50 J. S. Seol, S. Y. Lee, J. C. Lee, H. D. Nam and K. H. Kim, *Sol. Energy Mater. Sol. Cells*, 2003, **75**, 155–162.
51 H. Katagiri, N. Sasaguchi, S. Hando, S. Hoshino, J. Ohashi and T. Yokota, *Sol. Energy Mater. Sol. Cells*, 1997, **49**, 407–414.
52 H. Araki, A. Mikaduki, Y. Kubo, T. Sato, K. Jimbo, W. S. Maw, H. Katagiri, M. Yamazaki, K. Oishi and A. Takeuchi, *Thin Solid Films*, 2008, **517**, 1457–1460.
53 K. Oishi, G. Saito, K. Ebina, M. Nagahashi, K. Jimbo, W. S. Maw, H. Katagiri, M. Yamazaki, H. Araki and A. Takeuchi, *Thin Solid Films*, 2008, **517**, 1449–1452.
54 Y. B. K. Kumar, G. S. Babu, P. U. Bhaskar and V. S. Raja, *Phys. Status Solidi A*, 2009, **206**, 1525–1530.
55 Y. B. K. Kumar, G. S. Babu, P. U. Bhaskar and V. S. Raja, *Sol. Energy Mater. Sol. Cells*, 2009, **93**, 1230–1237.
56 H. Katagiri, K. Jimbo, W. S. Maw, K. Oishi, M. Yamazaki, H. Araki and A. Takeuchi, *Thin Solid Films*, 2009, **517**, 2455–2460.
57 Q. Guo, G. M. Ford, H. W. Hillhouse and R. Agrawal, *Nano Lett.*, 2009, **9**, 3060–3065.
58 D. Abou-Ras, G. Kostorz, D. Bremaud, M. Kalin, F. V. Kurdesau, A. N. Tiwari and M. Dobeli, *Thin Solid Films*, 2005, **480**, 433–438.
59 S. Y. Chen, X. G. Gong, A. Walsh and S. H. Wei, *Appl. Phys. Lett.*, 2010, **96**, 021902.
60 W. Haas, T. Rath, A. Pein, J. Rattenberger, G. Trimmel and F. Hofer, *Chem. Commun.*, 2011, **47**, 2050–2052.
61 H. Wei, W. Guo, Y. J. Sun, Z. Yang and Y. F. Zhang, *Mater. Lett.*, 2010, **64**, 1424–1426.
62 A. Shavel, J. Arbiol and A. Cabot, *J. Am. Chem. Soc.*, 2010, **132**, 4514.

63 B. Trauzettel, D. V. Bulaev, D. Loss and G. Burkard, *Nat. Phys.*, 2007, **3**, 192–196.
64 P. Hewageegana and V. Apalkov, *Phys. Rev. B: Condens. Matter Mater. Phys.*, 2008, **77**, 245426.
65 J. Guttinger, C. Stampfer, S. Hellmuller, F. Molitor, T. Ihn and K. Ensslin, *Appl. Phys. Lett.*, 2008, **93**, 212102.
66 F. Libisch, C. Stampfer and J. Burgdorfer, *Phys. Rev. B: Condens. Matter Mater. Phys.*, 2009, **79**, 115423.
67 J. Güttinger, T. Frey, C. Stampfer, T. Ihn and K. Ensslin, *Phys. Rev. Lett.*, 2010, **105**, 116801.
68 S. Schumacher, *Phys. Rev. B: Condens. Matter Mater. Phys.*, 2011, **83**, 081417.
69 J. Zhao, G. F. Chen, L. Zhu and G. X. Li, *Electrochem. Commun.*, 2011, **13**, 31–33.
70 H. G. Zhang, H. Hu, Y. Pan, J. H. Mao, M. Gao, H. M. Guo, S. X. Du, T. Greber and H. J. Gao, *J. Phys.: Condens. Matter*, 2010, **22**, 302001.
71 J. W. Li and V. B. Shenoy, *Appl. Phys. Lett.*, 2010, **98**, 013105.
72 G. Giavaras and F. Nori, *Appl. Phys. Lett.*, 2010, **97**, 243106.
73 C. D. Simpson, J. D. Brand, A. J. Berresheim, L. Przybilla, H. J. Räder and K. Müllen, *Chem.–Eur. J.*, 2002, **8**, 1424–1429.
74 D. Y. Pan, J. C. Zhang, Z. Li and M. H. Wu, *Adv. Mater.*, 2010, **22**, 734.
75 Y. Li, Y. Hu, Y. Zhao, G. Q. Shi, L. E. Deng, Y. B. Hou and L. T. Qu, *Adv. Mater.*, 2011, **23**, 776.
76 P. Rempala, J. Kroulik and B. T. King, *J. Am. Chem. Soc.*, 2004, **126**, 15002–15003.
77 I. P. Hamilton, B. Li, X. Yan and L.-s. Li, *Nano Lett.*, 2011, **11**, 1524–1529.
78 L. S. Li and X. Yan, *J. Phys. Chem. Lett.*, 2010, **1**, 2572–2576.
79 M. L. Mueller, X. Yan, J. A. McGuire and L. S. Li, *Nano Lett.*, 2010, **10**, 2679–2682.
80 X. Yan, X. Cui, B. S. Li and L. S. Li, *Nano Lett.*, 2010, **10**, 1869–1873.
81 J. Wu, W. Pisula and K. Mullen, *Chem. Rev.*, 2007, **107**, 718–747.
82 J. Wu, Z. Tomovic, V. Enkelmann and K. Mullen, *J. Org. Chem.*, 2004, **69**, 5179–5186.
83 I. L. Medintz, H. T. Uyeda, E. R. Goldman and H. Mattoussi, *Nat. Mater.*, 2005, **4**, 435–446.
84 S. Y. Chen, A. Walsh, Y. Luo, J. H. Yang, X. G. Gong and S. H. Wei, *Phys. Rev. B: Condens. Matter Mater. Phys.*, 2010, **82**, 195203.
85 S. Y. Chen, J. H. Yang, X. G. Gong, A. Walsh and S. H. Wei, *Phys. Rev. B: Condens. Matter Mater. Phys.*, 2010, **81**, 245204.
86 J. J. Wang, Y. Q. Wang, F. F. Cao, Y. G. Guo and L. J. Wan, *J. Am. Chem. Soc.*, 2010, **132**, 12218–12221.
87 P. Podsiadlo, G. Krylova, B. Lee, K. Critchley, D. J. Gosztola, D. V. Talapin, P. D. Ashby and E. V. Shevchenko, *J. Am. Chem. Soc.*, 2010, **132**, 8953–8960.
88 D. V. Talapin, J. S. Lee, M. V. Kovalenko and E. V. Shevchenko, *Chem. Rev.*, 2009, **110**, 389–458.
89 M. V. Kovalenko, M. Scheele and D. V. Talapin, *Science*, 2009, **324**, 1417–1420.
90 M. V. Kovalenko, M. I. Bodnarchuk, J. Zaumseil, J. S. Lee and D. V. Talapin, *J. Am. Chem. Soc.*, 2010, **132**, 10085–10092.
91 M. V. Kovalenko, B. Spokoyny, J. S. Lee, M. Scheele, A. Weber, S. Perera, D. Landry and D. V. Talapin, *J. Am. Chem. Soc.*, 2010, **132**, 6686–6695.
92 S. Wang, D. Yu and L. Dai, *J. Am. Chem. Soc.*, 2011, **133**, 5182–5185.
93 A. V. Ellis, M. R. Waterland and J. Quinton, *Chem. Lett.*, 2007, **36**, 1172–1173.
94 F. Cordella, M. De Nardi, E. Menna, C. Hebert and M. A. Loi, *Carbon*, 2009, **47**, 1264–1269.
95 D. M. Guldi, G. M. A. Rahman, N. Jux, D. Balbinot, U. Hartnagel, N. Tagmatarchis and M. Prato, *J. Am. Chem. Soc.*, 2005, **127**, 9830–9838.
96 J. Han, H. Kim, D. Y. Kim, S. M. Jo and S. Y. Jang, *ACS Nano*, 2010, **4**, 3503–3509.
97 J. L. Hernandez-Lopez, E. R. Alvizo-Paez, S. E. Moya and J. Ruiz-Garcia, *Carbon*, 2007, **45**, 2448–2450.
98 H. Isobe, T. Tanaka, R. Maeda, E. Noiri, N. Solin, M. Yudasaka, S. Iijima and E. Nakamura, *Angew. Chem., Int. Ed.*, 2006, **45**, 6676–6680.
99 L. W. Qu, L. M. Veca, Y. Lin, A. Kitaygorodskiy, B. L. Chen, A. M. McCall, J. W. Connell and Y. P. Sun, *Macromolecules*, 2005, **38**, 10328–10331.
100 R. Sainz, A. M. Benito, M. T. Martinez, J. F. Galindo, J. Sotres, A. M. Baro, B. Corraze, O. Chauvet and W. K. Maser, *Adv. Mater.*, 2005, **17**, 278.
101 B. Zhao, H. Hu and R. C. Haddon, *Adv. Funct. Mater.*, 2004, **14**, 71–76.
102 B. Zhao, H. Hu, A. P. Yu, D. Perea and R. C. Haddon, *J. Am. Chem. Soc.*, 2005, **127**, 8197–8203.
103 H. Masuda, K. Nishio and N. Baba, *Jpn. J. Appl. Phys.*, 1992, **31**, L1775–L1777.
104 C. Goh, K. M. Coakley and M. D. McGehee, *Nano Lett.*, 2005, **5**, 1545–1549.
105 J. Wang and Z. Q. Lin, *J. Phys. Chem. C*, 2009, **113**, 4026–4030.
106 J. M. Macak, H. Tsuchiya, L. Taveira, S. Aldabergerova and P. Schmuki, *Angew. Chem., Int. Ed.*, 2005, **44**, 7463.
107 G. K. Mor, O. K. Varghese, M. Paulose, K. Shankar and C. A. Grimes, *Sol. Energy Mater. Sol. Cells*, 2006, **90**, 2011–2075.
108 J. Wang and Z. Q. Lin, *Chem. Mater.*, 2008, **20**, 1257–1261.
109 J. Wang, L. Zhao, V. S. Y. Lin and Z. Q. Lin, *J. Mater. Chem.*, 2009, **19**, 3682–3687.
110 B. Liu and E. S. Aydil, *J. Am. Chem. Soc.*, 2009, **131**, 3985–3990.
111 B. Pradhan, S. K. Batabyal and A. J. Pal, *Sol. Energy Mater. Sol. Cells*, 2007, **91**, 769–773.
112 M. Paulose, K. Shankar, O. K. Varghese, G. K. Mor and C. A. Grimes, *J. Phys. D: Appl. Phys.*, 2006, **39**, 2498.
113 K. Shankar, G. K. Mor, H. E. Prakasam, S. Yoriya, M. Paulose, O. K. Varghese and C. A. Grimes, *Nanotechnology*, 2007, **18**, 065707.
114 J. Wang and Z. Q. Lin, *Chem. Mater.*, 2010, **22**, 579–584.
115 K. Zhu, N. R. Neale, A. Miedaner and A. J. Frank, *Nano Lett.*, 2007, **7**, 69–74.
116 K. Zhu, T. B. Vinzant, N. R. Neale and A. J. Frank, *Nano Lett.*, 2007, **7**, 3739–3746.
117 O. K. Varghese, M. Paulose and C. A. Grimes, *Nat. Nanotechnol.*, 2009, **4**, 592–597.
118 O. K. Varghese, D. Gong, M. Paulose, K. G. Ong and C. A. Grimes, *Sens. Actuators, B*, 2003, **93**, 338.
119 G. K. Mor, M. A. Carvalho, O. K. Varghese, M. V. Pishko and C. A. Grimes, *J. Mater. Res.*, 2004, **19**, 7.
120 O. K. Varghese, D. Gong, M. Paulose, K. G. Ong, E. C. Dickey and C. A. Grimes, *Adv. Mater.*, 2003, **15**, 624–627.
121 G. K. Mor, K. Shankar, M. Paulose, O. K. Varghese and C. A. Grimes, *Nano Lett.*, 2005, **5**, 191.
122 O. K. Varghese and C. A. Grimes, *Sol. Energy Mater. Sol. Cells*, 2008, **92**, 374–384.
123 O. K. Varghese, M. Paulose, K. Shankar, G. K. Mor and C. A. Grimes, *J. Nanosci. Nanotechnol.*, 2005, **5**, 1158–1165.
124 S. P. Albu, A. Ghicov, J. M. Macak, R. Hahn and P. Schmuki, *Nano Lett.*, 2007, **7**, 1286.
125 J. M. Macak, M. Zlamal, J. Krysa and P. Schmuki, *Small*, 2007, **3**, 300–304.
126 J. Park, S. Bauer, K. von der Mark and P. Schmuki, *Nano Lett.*, 2007, **7**, 1686.
127 J. Park, S. Bauer, P. Schmuki and K. von der Mark, *Nano Lett.*, 2009, **9**, 3157–3164.

